Shaping Ge Islands on Si(001) Surfaces with Misorientation Angle

L. Persichetti, A. Sgarlata, M. Fanfoni, and A. Balzarotti

Dipartimento di Fisica, Università di Roma "Tor Vergata", Via della Ricerca Scientifica,1-00133 Roma, Italy
(Received 19 November 2009; published 22 January 2010)

A complete description of Ge growth on vicinal Si(001) surfaces in the angular miscut range 0°–8° is presented. The key role of substrate vicinality is clarified from the very early stages of Ge deposition up to the nucleation of 3D islands. By a systematic scanning tunneling microscopy investigation we are able to explain the competition between step-flow growth and 2D nucleation and the progressive elongation of the 3D islands along the miscut direction [110]. Using finite element calculations, we find a strict correlation between the morphological evolution and the energetic factors which govern the {105} faceting at atomic scale.

Because of the potential applications in novel nanostructured devices [1,2], the Stranski-Krastanov growth of self-assembled islands in strained heteroepitaxial systems is a topic attracting ever-increasing interest. Since the seminal paper of Mo *et al.* [3], Ge on Si(001) has been widely used as a model system for handling the surprising complexity of heteroepitaxy. At present, combined experimental and theoretical efforts have elucidated the main mechanisms involved in the strain-driven transition to faceted Ge islands on the flat Si(001) surface, i.e., the continuous shape evolution from unfaceted prepyramids [4,5] via pyramidal huts bounded by {105} facets [6] to multifaceted domes and barns [7]. On the contrary, the experimental results available to date on vicinal Si(001) substrates are rather scattered and hardly amenable to a unified picture of the strain relaxation and nucleation path. On Si(001) surfaces with a 4° miscut in the [110] direction Teichert *et al.* [8] and Lichtemberger *et al.* [9] reported the appearance of triangular-shaped, asymmetric {105} faceted islands. On the 8°-miscut Si(001) surface, Szkutnik *et al.* [10] followed the Ge growth up to the formation of elongated {105}-faceted ripple structures. The same ripple morphology has been observed by Ronda *et al.* [11] and, more recently, by Sanduijav *et al.* [12] on a striped patterned substrate.

The aim of the present investigation is to provide a complete and unified description of Ge growth on vicinal Si(001). Our high-resolution scanning tunneling microscopy (STM) study proves that the substrate vicinality controls the transition from step-flow growth to 2D island growth as well as controlling the strain-induced evolution in shape and orientation of the 3D islands from square pyramids on the flat Si(001) surface to faceted ripples on high-miscut substrates. As shown by *ab initio* calculations [13,14], the {105} faceting lowers significantly the free energy of the system for compressive strained Ge. We find that, despite the considerably different morphology, the evolution of Ge islands is basically due to the stability of the {105} facets. We corroborate this assumption by a direct comparison between the predictions of a simple structural elastic model and a set of high-resolution STM images of Ge islands grown on Si(001) vicinal surfaces with different miscuts.

Experiments were carried out in an ultrahigh vacuum chamber ($p < 3 \times 10^{-11}$ torr) equipped with a variable temperature scanning tunneling microscope. We used Si(001) wafers with azimuthal angle $\phi = 0°$ and polar miscut angle θ ranging between 0° and 8° toward the [110] direction. The substrates were cleaned *in situ* by a standard flashing procedure at 1473 K [15]. Ge was deposited by physical vapor deposition at 873 K at constant flux of 5×10^{-2} ML/s. STM measurements were carried out at room temperature in the constant-current mode, using *W*-probe tips.

For Ge heteroepitaxy on the flat Si(001) substrate, in line with the pioneering work by Voigtlander [16], our investigation supports the picture of competition between step-flow growth and 2D-island nucleation. The clean substrate with alternating (2×1) and (1×2) reconstructed terraces is displayed in Fig. 1(a); the surface reconstruction is accompanied by dimerization along $\langle 110 \rangle$ directions and hence the dimer rows are orthogonal on terraces separated by an odd number of single-height steps. The deposition of 0.7 ML of Ge at first results in the formation of a periodic array of missing dimers which partially reduce the misfit strain [Fig. 1(b)] [17–19]. After deposition of 1.7 ML of Ge [Fig. 1(c)], the transition from pure step flow to 2D nucleation starts with the formation of islands selectively on the larger terraces, out of the capture zone of the step edges. At a coverage of 2.1 ML [Fig. 1(d)], further two-dimensional island nucleation occurs, together with the appearance of the ($M \times N$) wetting layer morphology; i.e., larger trenches of missing dimer rows form perpendicular to dimer vacancies [16].

Surface vicinality substantially changes the previous picture, since no 2D island nucleation occurs on misoriented substrates. As the miscut angle is increased from 0° to 2°, the average terrace width is reduced from 94 to

036104-1
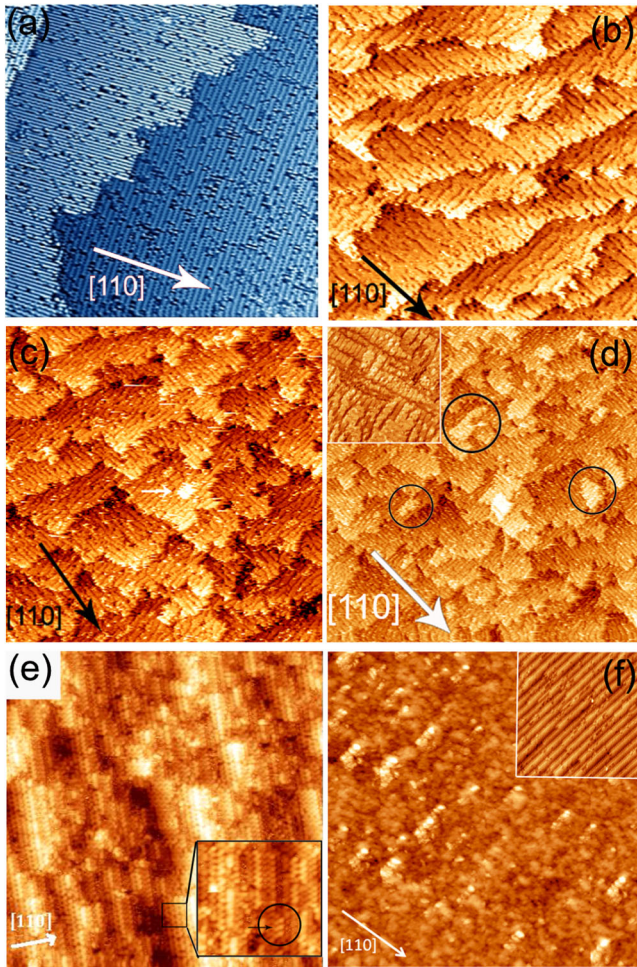
FIG. 1 (color online). STM images on Si(001): (a) (50×50 nm^2) flat clean surface. (b) (180×180 nm^2) 0.7 ML Ge on flat surface. (c) (300×300 nm^2) 1.7 ML Ge on flat surface. The white arrow points to a 2D island. (d) (300×300 nm^2) 2.1 ML Ge on flat surface. Circles show 2D islands. In the inset (70×70 nm^2) the ($M \times N$) reconstruction is displayed. (e) (50×50 nm^2) 0.4 ML Ge on a 4°-miscut surface. In the inset (20×20 nm^2) the $p(2 \times 2)$ reconstruction is highlighted (circle). (f) (300×300 nm^2) 1.4 ML Ge on a 6°-miscut surface. In the inset (40×40 nm^2) steps on the clean surface are shown as reference. In each panel the [110] miscut direction is indicated.

6.8 nm [20]. The latter values have to be compared with the effective surface Ge diffusion length on Si(001), $L = (D/R)^{1/4}$, where D is the diffusion coefficient of Ge adatoms [21] and R is the deposition rate. At the deposition temperature of 873 K, the effective diffusion length is approximately 20 nm; thus, the diffusing adatoms reach the step edges before the formation of critical nuclei. This is consistent with STM images at 4°- and 6°-miscut angles [Figs. 1(e) and 1(f)]. In both cases, a pure step flow takes place and no 2D island nucleation occurs on terraces. On the 4°-miscut surface, at submonolayer coverage, atomic steps are bunched together because of the step-flow mecha-

nism [Fig. 1(e)]; the appearance of the $p(2 \times 2)$ reconstruction, shown in the inset of Fig. 1(e), was theoretically predicted [22] and associated to an intermixing process [23]. Similarly, at a miscut angle of 6° and 1.4 ML of coverage, the incorporation of Ge adatoms at the step edge promotes the progressive formation of Ge chains, which preferentially decorate step edges [Fig. 1(f)]. These chains are expected to drive the evolution to 3D structures in the coverage range 3.5–4 ML, as already observed on vicinal surfaces with an 8° miscut [10].

While the different 2D growth modes on vicinal substrates can be fully explained through a simple kinetic model comprising surface diffusion processes at a miscut-dependent length scale, the three-dimensional growth depends, in principle, on a complex interplay between kinetics and thermodynamics, this resulting from an intriguing mixture of effects (stress-induced faceting, step-edge barrier to diffusion, alloying,...etc.). In this composite framework, the following experimental findings make it possible to fix the key-features of the 3D-growth on the basis of energetic considerations only.

Figure 2(a) shows STM images of Ge faceted pyramids on the flat Si(001) surface. The island base is almost square with each side oriented along the [100] direction forming a 45° angle to the direction of the dimer rows on the ($M \times N$) reconstructed wetting layer [inset in the top-left corner of Fig. 2(a)]. The dominant surface orientations can be directly extracted from the surface orientation map (SOM) of STM images [24]. The four peaks in the SOM, shown in the inset of Fig. 2(a), correspond to the characteristic {105} facets which bind the pyramids. When growing on a substrate misoriented by 1.5°, the Ge pyramids become elongated into the miscut [110] direction [Fig. 2(b)], but still {105} faceted [inset Fig. 2(b)]. The island elongation increases as the miscut angle gets higher, as evident in the miscut range 2°–6° [Figs. 2(c), 2(d), 3(a), and 3(b)]. This progressive shape transition is accompanied with the increase of surface area of the facets along the step-down direction at the expense of the other two facets.

Our experimental results suggest that the driving force for the morphological evolution in the island shape and orientation is the {105} facet stability. Previous works have demonstrated that the formation of the {105} facets on the flat Si(001) surface is accompanied by an effective strain relief that overcompensates the increase in surface energy [13,14]. To understand whether the substrate vicinality might change this scenario, we have evaluated the free energy E_{tot} of an island grown on the 6°-Si(001) surface with respect to a flat layer, as a function of its volume and shape [Fig. 4(a)]. According to Tersoff and LeGoues [25], E_{tot} consists of a surface energy term, due to the creation of additional surfaces, and a relaxation energy term, which includes both the elastic energy in the dot and the extra elastic energy in the substrate. The strain energy relaxation is computed by finite element (FEM) calculations [26]. We
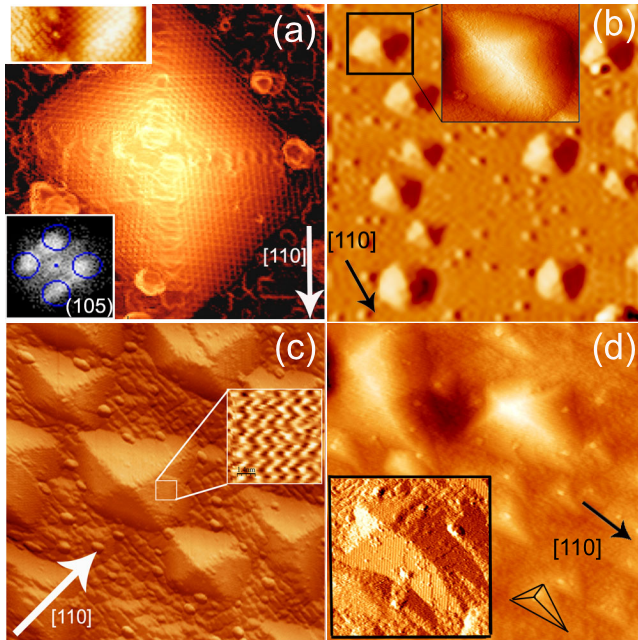
FIG. 2 (color online). STM images of pyramidal huts on the Si(001) surface with increasing miscut angle: (a) $(50 \times 50 \text{ nm}^2)$ 9 ML Ge on flat Si(001). In the top-left corner an enlarged view $(22 \times 9 \text{ nm}^2)$ shows the reconstruction of the {105} facets forming a 45° angle with the dimer rows on the $(M \times N)$ reconstructed wetting layer. In the bottom-left corner, the SOM is reported. The {105} peaks are marked by circles. (b) $(1100 \times 1100 \text{ nm}^2)$ 3 ML Ge on 1.5°-miscut Si(001). In the inset $(100 \times 100 \text{ nm}^2)$ a hut is displayed. (c) $(145 \times 145 \text{ nm}^2)$ 3 ML Ge on 2°-miscut Si(001). The rebonded-step reconstruction of the facets is highlighted [28]. (d) $(230 \times 230 \text{ nm}^2)$ 3 ML Ge on 4°-miscut Si(001). In the inset $(80 \times 80 \text{ nm}^2)$ a single pyramid is shown in derivative mode. Note new layers growing on the facets. The geometrical shape of the pyramids is highlighted.

FIG. 3 (color online). STM images: (a) $(150 \times 150 \text{ nm}^2)$ 3 ML Ge on 6°-miscut Si(001). (b) $(100 \times 100 \text{ nm}^2)$ 3 ML Ge on 6°-miscut Si(001). Note the wetting layer reconstruction together with the morphology of the uncompleted facets along the step-down direction. (c) $(400 \times 400 \text{ nm}^2)$ 6 ML Ge on 8°-miscut Si(001). In the inset an enlarged view $(140 \times 140 \text{ nm}^2)$ shows the ripple-zipping mechanism. (d) $(40 \times 40 \text{ nm}^2)$ 9 ML Ge on 8°-miscut Si(001).

note [Fig. 4(a)] that the {105} pyramids display the lowest energy for volumes less than 290 nm³, which is the same volume as in our experimental data. Therefore, consistent with STM nanotopography, {105} facets are energetically favored even in the case of growth on misoriented Si(001) substrates. In other words, the extra free energy of vicinal surfaces is negligible. This result allows us to explain with a geometrical model the measured island shape evolution. As already reported [10], in a pyramid the [551] intersection line of adjacent {105} facets forms a 8.05° angle with the (001) plane. To allow {105} faceting, this angle must never change, producing the observed elongation toward the miscut direction, as schematically illustrated in Fig. 4(b). In order to see how far this hypothesis matches the experiment and to quantify the miscut-dependent asymmetry of the dots, we have measured the ratio between the longest and the shortest island side. In Fig. 4(c), this ratio's values, extracted from STM images, are compared with the expected analytical ratio in an ideal (105)

pyramid on vicinal substrates. The match with the experiment is impressive.

Once the overall picture has been defined, the special situation for miscuts around 8° becomes perfectly clear. When the miscut angle equals the aforementioned 8.05° angle, a pyramidal shape can no longer form, since the [551] intersection line should run parallel to the substrate orientation [schematic draws in Figs. 4(c) and 4(d)]; thus, the system rearranges itself into ripples, as shown in the Figs. 3(c) and 3(d). By FEM calculations, we find that this rippled structure allows a significant elastic strain relief, as shown in Fig. 4(d), which displays the island elastic energy density for each miscut angle. We observe that, while at 6 ML the (105) domains still coexist with (001)-faceted wetting layer [10], at 9 ML [Fig. 3(d)] the surface is completely (105) faceted. Note the occurrence of a ripple-zipping mechanism [27], where different ripples meet [inset Fig. 3(c)].

In conclusion, we have reported a complete picture which provides new insights into the microscopic growth mechanisms on vicinal surfaces. A broad range of experimental observations has been compared to finite element model predictions of the stress energy distribution. Although the complex miscut-dependent nature of vicinal surfaces exhibits distinctive properties compared to an ideal flat surface, we have identified in the {105} energetics
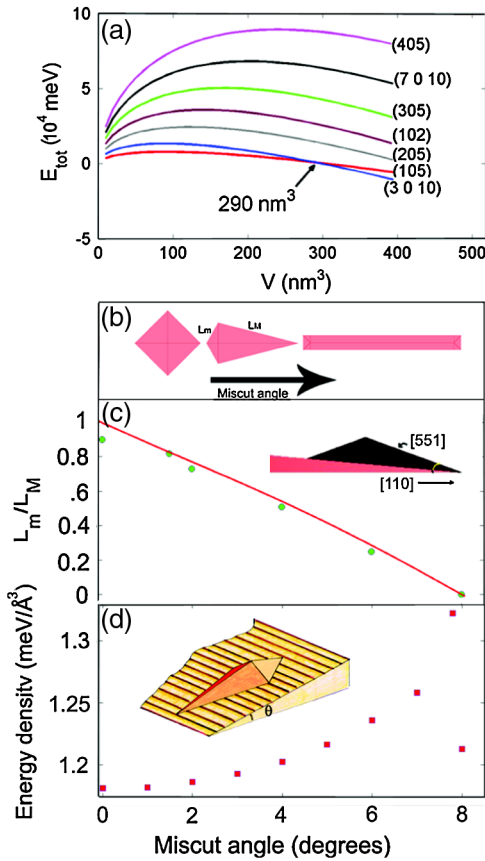
FIG. 4 (color online).   (a) FEM free energy of an island grown on the 6°-Si(001) surface, with respect to a flat layer. The Miller indexes indicate the respective facet orientation for each curve. The arrow points at the maximum volume for which the {105} pyramid is stable. (b) Schematic illustration of the shape transition in Ge islands as a function of the miscut angle. L_m and L_M are the shortest and the longest island side, respectively. (c) (L_m/L_M) ratio as a function of the miscut angle. The filled dots are the experimental values measured from STM images, while the continuous line represents the calculated ratio for an ideal (105) pyramid. The schematic drawing displays the angle between the [551] intersection line of adjacent {105} facets and the vicinal substrate orientation. (d) Elastic energy density computed by FEM calculations for the different Ge island shapes observed on the vicinal Si(001). Both the elastic energy in the dot and the extra elastic energy in the substrate are taken into account. The sudden decrease at the 8° miscut refers to a ripple closed by low index facets in the miscut direction.

the leading mechanism which drives the heteroepitaxial growth. The significant free energy gain due to the {105} faceting reduces the problem of dot shapes to a matter of geometry.

[1] D. Bimberg, J. Phys. D **38**, 2055 (2005).
[2] N. L. Rowell, D. J. Lockwood, I. Berbezier, P. D. Szkutnik, and A. Ronda, J. Electrochem. Soc. **156**, H913 (2009).
[3] Y.-W. Mo, D. E. Savage, B. S. Swartzentruber, and M. G. Lagally, Phys. Rev. Lett. **65**, 1020 (1990).
[4] A. Vailionis, B. Cho, G. Glass, P. Desjardins, David G. Cahill, and J. E. Greene, Phys. Rev. Lett. **85**, 3672 (2000).
[5] A. Rastelli, H. Von Känel, B. J. Spencer, and J. Tersoff, Phys. Rev. B **68**, 115301 (2003).
[6] J. Tersoff, B. J. Spencer, A. Rastelli, and H. von Känel, Phys. Rev. Lett. **89**, 196104 (2002).
[7] F. Montalenti *et al.*, Phys. Rev. Lett. **93**, 216102 (2004).
[8] C. Teichert, J. C. Bean, and M. G. Lagally, Appl. Phys. A **67**, 675 (1998).
[9] H. Lichtenberger, M. Mühlberger, and F. Schäffler, Appl. Phys. Lett. **86**, 131919 (2005).
[10] P. D. Szkutnik, A. Sgarlata, A. Balzarotti, N. Motta, A. Ronda, and I. Berbezier, Phys. Rev. B **75**, 033305 (2007).
[11] A. Ronda and I. Berbezier, Physica E (Amsterdam) **23**, 370 (2004); I. Berbezier and A. Ronda, Surf. Sci. Rep. **64**, 47 (2009).
[12] B. Sanduijav, D. Matei, G. Chen, and G. Springholz, Phys. Rev. B **80**, 125329 (2009).
[13] V. B. Shenoy, C. V. Ciobanu, and L. B. Freund, Appl. Phys. Lett. **81**, 364 (2002).
[14] G. H. Lu, M. Cuma, and F. Liu, Phys. Rev. B **72**, 125415 (2005); G. H. Lu and F. Liu, Phys. Rev. Lett. **94**, 176103 (2005).
[15] A. Sgarlata, P. D. Szkutnik, and A. Balzarotti, Appl. Phys. Lett. **83**, 4002 (2003).
[16] B. Voigtländer, Surf. Sci. Rep. **43**, 127 (2001).
[17] U. Köhler, O. Jusko, B. Müller, M. Horn-von-Hoegen, and M. Pook, Ultramicroscopy **42–44**, 832 (1992).
[18] F. Wu and M. G. Lagally, Phys. Rev. Lett. **75**, 2534 (1995).
[19] B. Voigtländer and M. Kästner, Phys. Rev. B **60**, R5121 (1999).
[20] L. Persichetti, A. Sgarlata, M. Fanfoni, M. Bernardi, and A. Balzarotti, Phys. Rev. B **80**, 075315 (2009).
[21] H. J. Kim, Z. M. Zhao, J. Liu, V. Ozolins, J. Y. Chang, and Y. H. Xie, J. Appl. Phys. **95**, 6065 (2004).
[22] S. M. Lee, E. Kim, Y. H. Lee, and N. G. Kim, J. Korean Phys. Soc. **33**, 684 (1998).
[23] X. R. Qin, B. S. Swartzentruber, and M. G. Lagally, Phys. Rev. Lett. **84**, 4645 (2000).
[24] The position of each spot represents the local normal orientation relative to the center, which corresponds to the (001) plane, while the intensity represents the relative amount of the surface with that orientation.
[25] J. Tersoff and F. K. LeGoues, Phys. Rev. Lett. **72**, 3570 (1994).
[26] We used the commercial COMSOL MULTIPHYSICS package as a FEM solver.
[27] J. Mysliveček, C. Schelling, F. Schäffler, G. Springholz, P. Šmilauer, J. Krug, and B. Voigtländer, Surf. Sci. **520**, 193 (2002).
[28] P. Raiteri, D. B. Migas, L. Miglio, A. Rastelli, and H. von Känel, Phys. Rev. Lett. **88**, 256103 (2002).